

Diagenetic Evolution and its Link to Poroperm Development in Paleozoic Carbonates of Cat Ba Island in Northeast Vietnam

Ly Thi Dieu Nguyen*

Petroleum Geoscience Program, Department of Geology,
Faculty of Science, Chulalongkorn University, Bangkok, 10330, Thailand
*Corresponding author email: nguyendieuly0612@gmail.com

Abstract

The study focuses on the diagenetic development of Paleozoic carbonate rocks on the Cat Ba island-Northeast Vietnam, via the integration of outcrop study, especially fracture cements, and isotopic analysis. From the C-O isotope plot, there are two distinct trends: 1) burial trend and 2) meteoric mixing trend. Paleozoic limestone in Cat Ba island experienced a consistent set of burial re-equilibration processes preserving remnants of a very early stage of burial, until the oxygen isotope values of veins and matrix calcites reached around -12‰. Around this value, the permeability of matrix is lost. The rocks can be later fractured to create pathways for fluid during uplift or subsequent deformations. Most fractures formed after the loss of matrix permeability are linked to Tertiary strike-slip displacement, which created three main fracture orientations: NE-SW, NW-SE and NNE-SSW. A meteoric mixing trend is preserved in calcites cement infilling in these fractures and their associated speleothems. Their isotope plot outlines two groups: 1) flowstones precipitated from bicarbonate-rich water coming from dissolved limestone at depth; 2) precipitation from fluid-dominant soil waters, which indicates the influence of shallow meteoric groundwater supplying most of the bicarbonate ions (Moore, 2001). When compared with a similar study of outcrops in Thuy Nguyen district (80 km away), the results show similar trends, which indicates potential regional application. Techniques used in this studies can be combined with other conventional reservoir characterization techniques to better understand diagenesis-related poroperm development in carbonate basement play, especially in the Gulf of Tonkin.

Keywords: Cat Ba island, Paleozoic carbonate, C-O isotope plot, diagenetic evolution

1. Introduction

Devonian to Permian carbonate is exposed in Cat Ba island, Hai Phong Province, Northeast Vietnam, and offers excellent outcrop analogs to carbonate buried hill plays in offshore Vietnam. There are few published studies of carbonates of the Cat Ba island, so the main purpose of this study is to investigate the impact of diagenesis on the reservoir quality evolution of in Devonian–Permian carbonate in this part of Northeast Vietnam.

This has been achieved by the integration of field observations and in-lab XRD, isotope and thin section analysis applied to four fresh outcrops on the Cat Ba island (Fig 1). Interpreting the calcite-filled fracture system and any diagenetic overprint will give a better understanding of structural and diagenetic evolution in the studied area and its link to poroperm.

2. Geological Setting

The Cat Ba island is divided into two main structural-stratigraphic associations: 1) Devonian-Carboniferous-Permian and 2) Cenozoic, which are separated by an unconformity (Tri et al, 2003) (Fig. 1). Overall, rocks on Cat Ba island form an anticlinorium consisting of alternating anticlines and synclines with a constant axis direction of NW-SE. Together with folding, faulting activity is clear in outcrop and complicates the fold structure as well as influencing the island's topographic development. The three main fault systems are visible on the island trending NE-SW, NW-SE and sub-E-W (Tri et al., 2003).

The first fault system trends NE-SW direction and is associated with the Yanshanian orogeny, which started in the Cretaceous (90 Ma). The second fault system trends NW-SE and is associated with the Himalayan orogeny since the Eocene (40 Ma) until the present. This is the

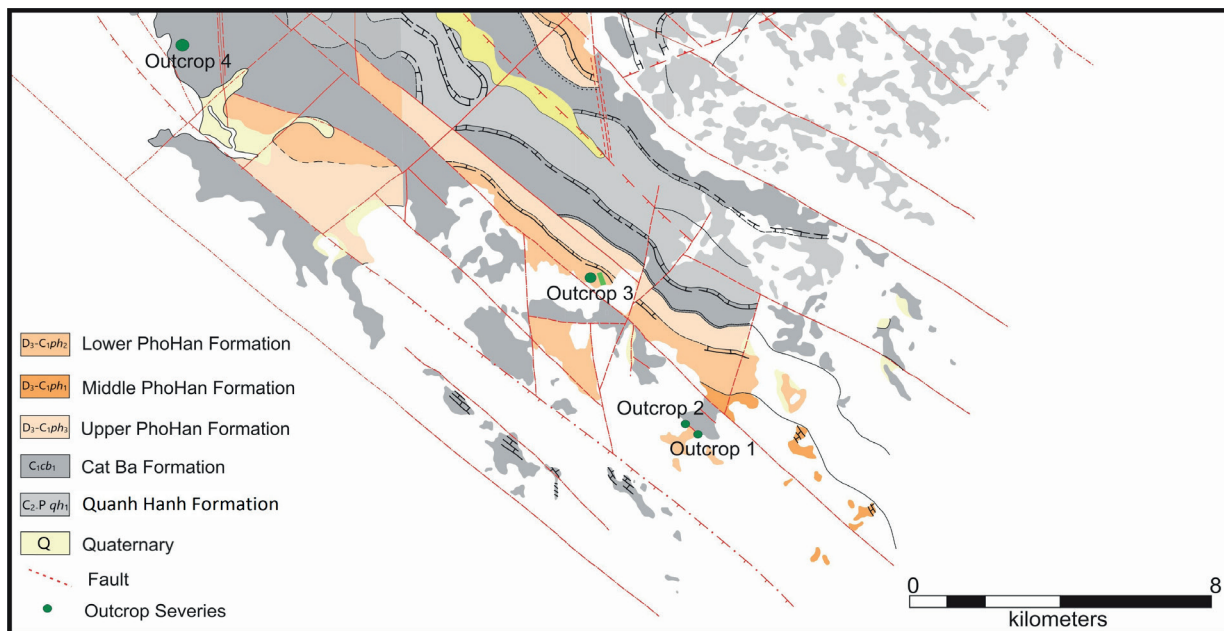


Figure 1. Geological map (scale 1:50,000) of Cat Ba island (Modified from GDGMV, 1993).

principal fault system of the Cat Ba island, which creates many of the structural deformation features noted in this study and includes slickensides and stratigraphic displacement across fault planes. The third fault system is oriented sub-E-W and relates to the present geological setting. Compared with the intense tectonic effects of previous faults, sub-E-W faulting is not significant but it does locally control the geological structure in the Cat Ba island. Along with this fault system, many smaller faults are visible which locally changes the tectonic expression of Cat Ba island (Nguyen et al., 2008).

3. Methodology

Methods used to generate the data for this study encompass both field work and laboratory work. Four fresh outcrops in Cat Ba island are investigated in the field, this involved describing geological characteristics and relationships, as well as measuring the fracture orientation and style (Fig. 1).

For laboratory work, by using a dental drill, 15 thin section and XRD samples are selected from the face of slabbed rocks from Cat Ba island. The position of XRD drilled points are identified on corresponding thin sections, then XRD results can help to confirm and name the mineralogy ascertained from stained thin section

analysis and also define other additional mineral components that cannot be determined based on thin section study.

Each thin section is divided into two parts: unstained and stained. For staining of the thin sections, Alizarin red-S and potassium ferricyanide dissolved in a dilute hydrochloric acid solution are used. By using this method, calcite, ferroan calcite, and ferroan dolomite (ankerite) are easily identifiable (Hitzman, 1999). All the stained thin section results are combined with XRD data to examine the rock type, matrix, shape and orientation, internal structures, timing and nature of calcite cement that filled the veins.

Beside thin sections, 111 isotope samples are taken from calcite cements and veins in order to understand the history of the various textures and lithologies, as well as the origin and timing of both matrix and the calcite-filled fractures. All drill powders are collected and clearly labeled before sending to the isotope lab at Monash University in Australia, followed by $\delta^{18}\text{O}$ and $\delta^{13}\text{C}$ analysis utilizing techniques outlined by Allegre (2008). The resulting oxygen isotope values ($\delta^{18}\text{O}_{\text{PDB}}$) become increasingly negative with burial, which reflects the change in rock-fluid re-equilibration as fluid temperature increases (Hoef, 2009). The measured $\delta^{18}\text{O}$ also are

an indicator of relative pore fluid temperature, less negative oxygen values on a C–O burial curve indicates cooler pore fluid, more negative values indicate warmer pore fluid. The carbon isotope value ($\delta^{13}\text{C}_{\text{PDB}}$) depend on the CO_2 amount derived from an organic source. They become more negative with increased organic carbon in the bicarbonate precipitated in the calcite. This organic carbon can come from a soil gas or catagenic source. The data is converted and compiled using a PDB standard matrix ($\delta^{13}\text{C}$ and $\delta^{18}\text{O}$ are both given in ‰PDB) and plotted in a single crossplot, which shows distinct but related C–O trends (Fig. 6A). In this study, the diagenetic terms such as eogenetic, mesogenetic and telogenetic are used following Choquette and Pray (1970) and illustrate early marine, burial and uplift related porosity changes.

4. Results

4.1 XRD analysis

The result from 15 selected samples show that calcite (CaCO_3) is the dominant mineral type in Cat Ba island carbonates with sub-dominant quartz (SiO_2) in one sample and some traces of muscovite ($\text{KAl}_2\text{Si}_3\text{AlO}_{10}(\text{OH})_2$), kaolinite ($\text{Al}_2\text{Si}_2\text{O}_5(\text{OH})_4$) and goethite (FeOOH). A

summary of XRD results is given in the table 1.

4.2 Outcrop, petrographic and isotopic analysis Outcrop 1

The first study outcrop (Fig. 2A) ($20^{\circ}42'58''\text{N}, 107^{\circ}03'02''\text{E}$) is a fresh beach-cliff outcrop near Cat Co beach which is some 100m long composed of strongly folded dark gray layer of upper Devonian-Carboniferous Pho Han Formation carbonate (Fig. 2A, 2B, 2C). There are many calcite veins, tension gashes (Fig. 2D) and vugs where the calcite veins show two main directions trending NE-SW and NW-SE (Fig. 2E), which is consistent with the two regional fault systems that overprint the study area.

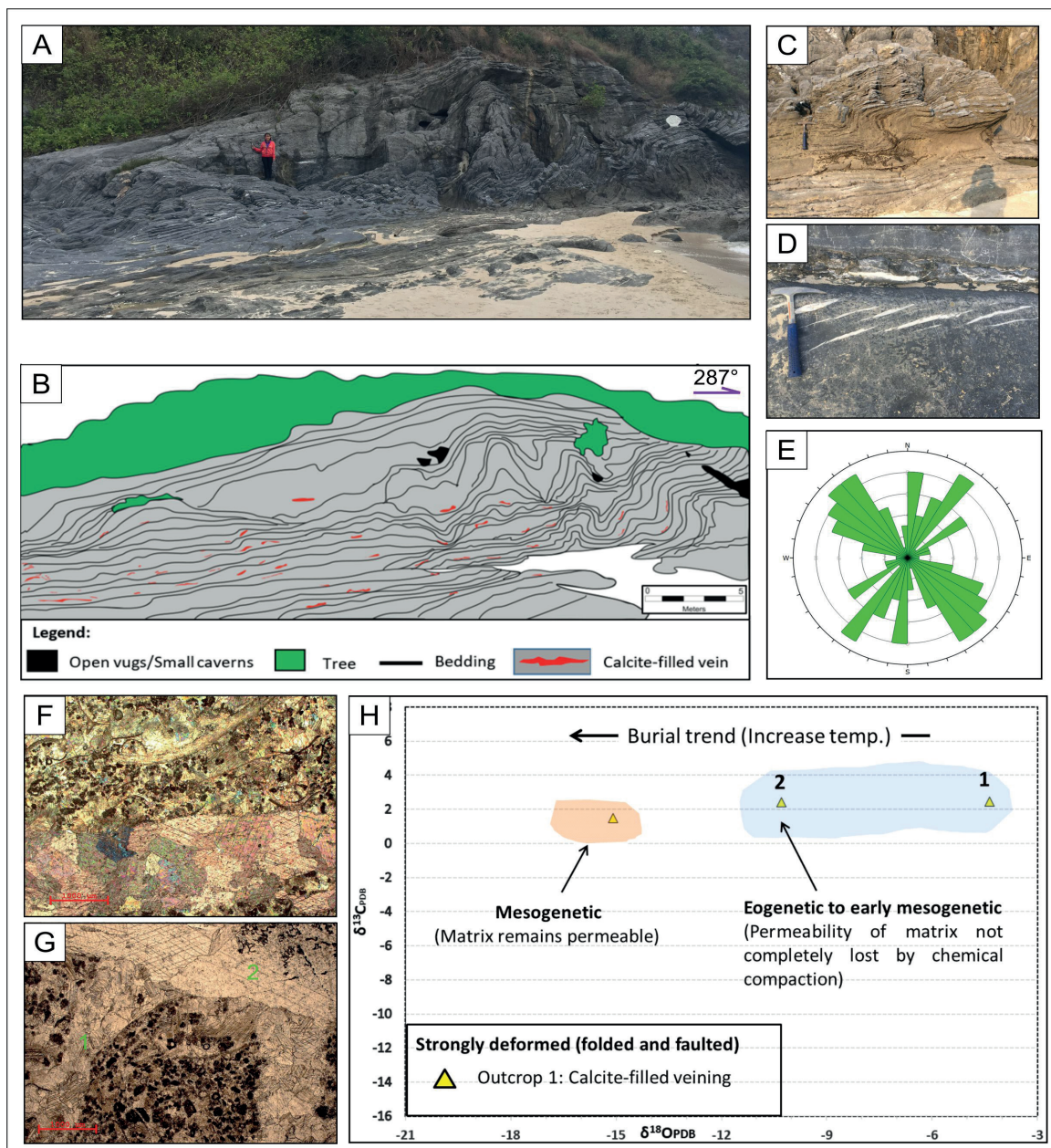
Outcrop 1 is a designated heritage site, therefore only 1 representative thin section is collected from the very thin laminated turbidite limestone. Petrography indicates a wackestone which contains a considerable amount of carbonate allochems, mainly foraminifera, algal debris, brachiopod and crinoid fragments that are floating in a calcite-cemented matrix (Fig. 2F). Most fragments of the fossils are deformed and dissolved by pressure solution during compaction and replaced by microsparite/or

Mineral Name	Composition	Relative abundance														
		1	2	3	4	5	6	7	8	9	10	11	12	13	14	15
Calcite	CaCO_3	D	D	D	D	D	D	D	D	D	D	D	D	D	D	D
Quartz	SiO_2														SD	
Muscovite	$\text{KAl}_2\text{Si}_3\text{AlO}_{10}(\text{OH})_2$														Tr-A	
Kaolinite	$\text{Al}_2\text{Si}_2\text{O}_5(\text{OH})_4$							Tr								
Goethite	FeOOH														Tr	
Semiquantitative Abbreviations:																
D = Dominant. Used for the component apparently most abundant, regardless of its probable percentage level																
SD = Sub-dominant. The next most abundant components(s) providing its percentage level is judged above about 20.																
A = Accessory. Components judged to be present between the levels of roughly 5 and 20%																
Tr = Trace. Components judged to be below about 5%.																

Table 1. XRD results from selected samples

micritic calcite. The rock has undergone extensive fracturing and folding, with most of fractures filled with sparry calcite (Fig. 2G). The C-O crossplot of the calcite-filled fractures (Fig. 2H) show isotopic evolution with a general trend of increasingly negative oxygen and carbon values. Two fracture trends are observed on the

slabbed sample: Fracture no.1 has a NE-SW strike direction, while fracture no.2 has a NW-SE direction (Fig. 2G). From these calcite-filled fractures, two isotope powder samples are drilled and the result is plotted on a C-O isotope plot (Fig. 2H). Values from NW-SE-oriented fractures have higher negative oxygen values than NE-SW



fractures which indicate the calcite with a NW-SE orientation precipitated from fluids with higher temperatures than the NE-SW calcite-filled fracture in this outcrop.

Outcrop 2

The second outcrop (Fig. 3A, 3B) ($20^{\circ}42'57''N$, $107^{\circ}03'54''E$) consists of some 200 m thick interval of upper Devonian to Carboniferous Pho Han Formation limestone,

marl, shale and chert with individual bed thickness ranging from 10-50 cm. According to the Vietnamese 1:50,000 geological map, these rocks belong to the Pho Han Formation. This outcrop contains gray micritic limestone, which consists mainly of bioclastic and intraclastic packstone. Bioclasts visible in thin section include brachiopods, gastropods and ostracod shells, crinoid stems and foraminiferal elements (Fig. 3E, 3F) that together construct a grain-supported

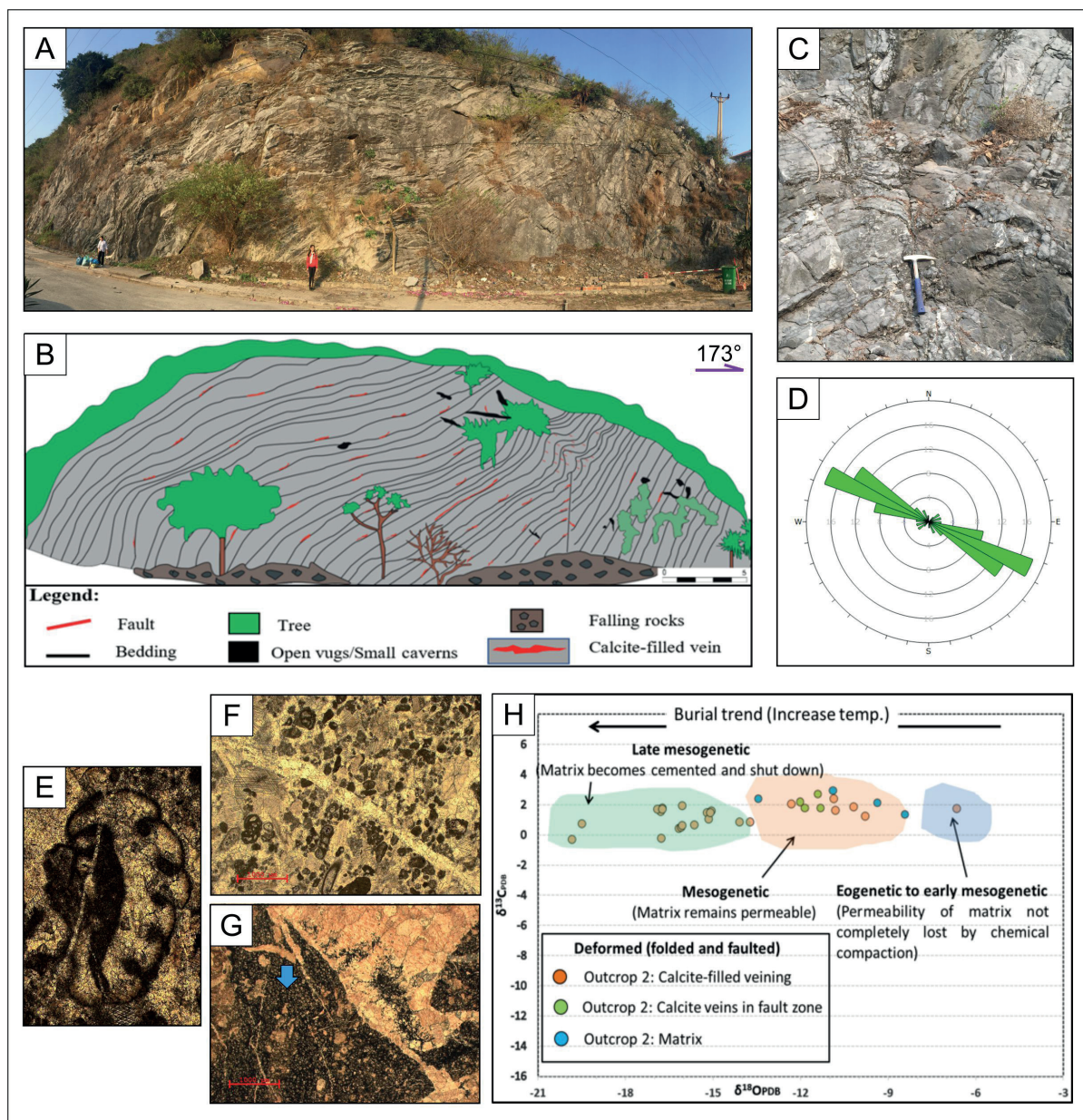
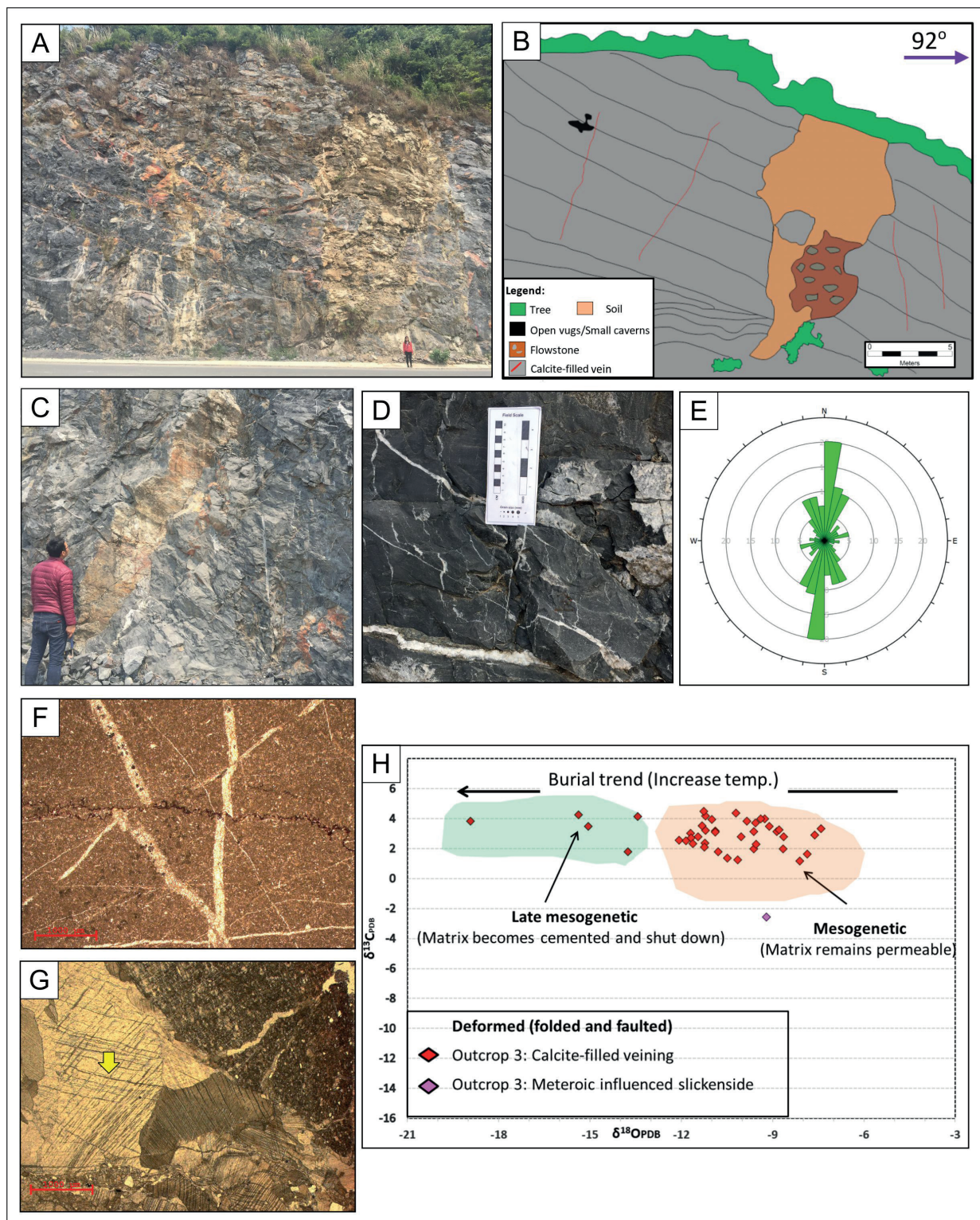


Figure 3. A) and B) Geological overview of outcrop 2 and the sketch shows the carbonate bedding orientation and the major features such as vugs, caves and calcite veins. C) Fault zone is observed D) Rose plot shows the orientation of calcite veins and fractures in outcrop 2 is toward WNW-ESE direction. E) Foraminifera. F) Crinoid stems and foraminifera are a part of bioclastic which defined as packstone. G) Dolomite within organic matter (blue arrow). H) C-O isotope plot shows sample values which are collected from outcrop 2.



packstone. Locally, euhedral and subhedral rhombic dolomite crystals within organic matter are seen (blue arrow) (Fig. 3G). The dominant calcite-filled fractures measured in this study show a WNW-ESE strike direction (Fig. 3D).

Isotopic signatures from outcrop 2 show an on-going C-O covariant trend (Fig. 3H) indicative of burial passing likely into deformation (based on comparison with the burial data in Warren et al., 2014). The matrix is likely still permeable in the early stages of calcite precipitation, as matrix and vein calcite continued to re-equilibrate due to interaction with increasingly warmer pore fluids. It stops when reaching to $\delta^{18}\text{O}$ value of -8‰ to -10‰ (shaded blue), then under the burial pressures and temperature equivalent to $\delta^{18}\text{O}$ value of -12‰ to -14‰, the matrix becomes cemented even in the inactive fault zones. In this studied outcrop, the $\delta^{18}\text{O}$ values are found greater than -12‰ to -14‰ (up to -20‰) (shaded green). It shows that hot fluid can still ingress and precipitate inside NW-SE fractures that are opened by fault and results in the further loss of residual matrix permeability.

Outcrop 3

The third outcrop ($20^{\circ}44'27''\text{N}$, $107^{\circ}01'40''\text{E}$) is roughly 11 km to the Northwest of the first outcrop and is a fresh roadcut that exposes the upper Devonian to Carboniferous Pho Han Formation. This outcrop is characterized by 0.5- 1.5 m thick limestone layers with a 10 m thick breccia (Fig. 4A, 4B). These beds strike WNW-ESE and dip to NNE. Both open and filled fractures are recorded at this site and show a dominant trend of NNE-SSW (Fig. 4E). The dominant lithology consists of crystalline mudstone which is typically ultrafine with uniform texture. The rock experienced tectonic activity, which is illustrated by sparry calcite filled fractures (yellow arrow) (Fig. 4G) and visible vugs and stylolites from thin sections (Fig. 4F). The mudstone contains few bioclasts.

The isotopic signature of calcite vein cements and a slickenside from outcrop 3 show typical early burial trend signatures with increasingly negative oxygen values related to increasing

burial temperature in the precipitating fluids (Fig. 4H). Most of the oxygen in the sampled veins show a spread of values from -7‰ to -12‰ (shaded brown) (Fig. 4H) and a second plot field with values increasingly negative up to -19‰ (shaded green).

The spread on the main group (shaded brown) stops on reaching the burial pressures and temperature equivalent to $\delta^{18}\text{O}$ value of -12‰, this likely indicates the matrix became cemented and shut down further fluid flow until the matrix is re-opened by fracturing during a later warmer deformation event(s). This is indicated by oxygen isotope values greater than -12‰ to -14‰ (up to -20‰). It demonstrates that fluid still ingress and precipitate inside fractures that are opened by fault and also show the loss of matrix permeability (Warren et al., 2014).

Outcrop 4

In outcrop 4 ($20^{\circ}46'33''\text{N}$, $106^{\circ}58'03''\text{E}$), the lower Carboniferous Cat Ba formation is exposed some 50 m thick and 200 m long and made up of mainly blocky light gray limestone beds that preserve abundant fractures and faults as a result of tectonic activity in this area. Furthermore, this outcrop is also marked by 5 m thick deformed and brecciated dolostone interval (Fig. 5A, 5B). Both open and filled fractures are recorded and show dominant trend of NW-SE with a minor NE-SW direction (Fig. 5E).

The dominant lithologies in outcrop 4 are crystalline mudstones. They are commonly pervasively overprinted by sparite or microsparite. In this outcrop, fewer fossils can be observed. The rock has been fractured, and the fractures typically contain residual organic matter (dark color in thin section) or sparry calcite (green arrow) (Fig. 5F). In addition, earlier textures are overprinted by both burial related calcite infilling vugs and by a variety of vein cements. In this outcrop, there are also a set of modern speleothems exposed within a 1-2 m diameter cavern that is filled by a combination of infiltrated soil and flowstone (Fig. 5C, 5D). The isotopic signatures show two distinct trends; 1) a burial trend and 2) a meteoric mixing trend (Fig. 5H). The sample matrix signature is bimodal

while calcite vein cement and slickensides tend to follow burial trend in the C-O crossplot, which indicates rock-fluid re-equilibration along a diagenetic passage into deeper burial, from the

eogenetic to mesogenetic cement (Moore, 2011; Warren et al., 2014).

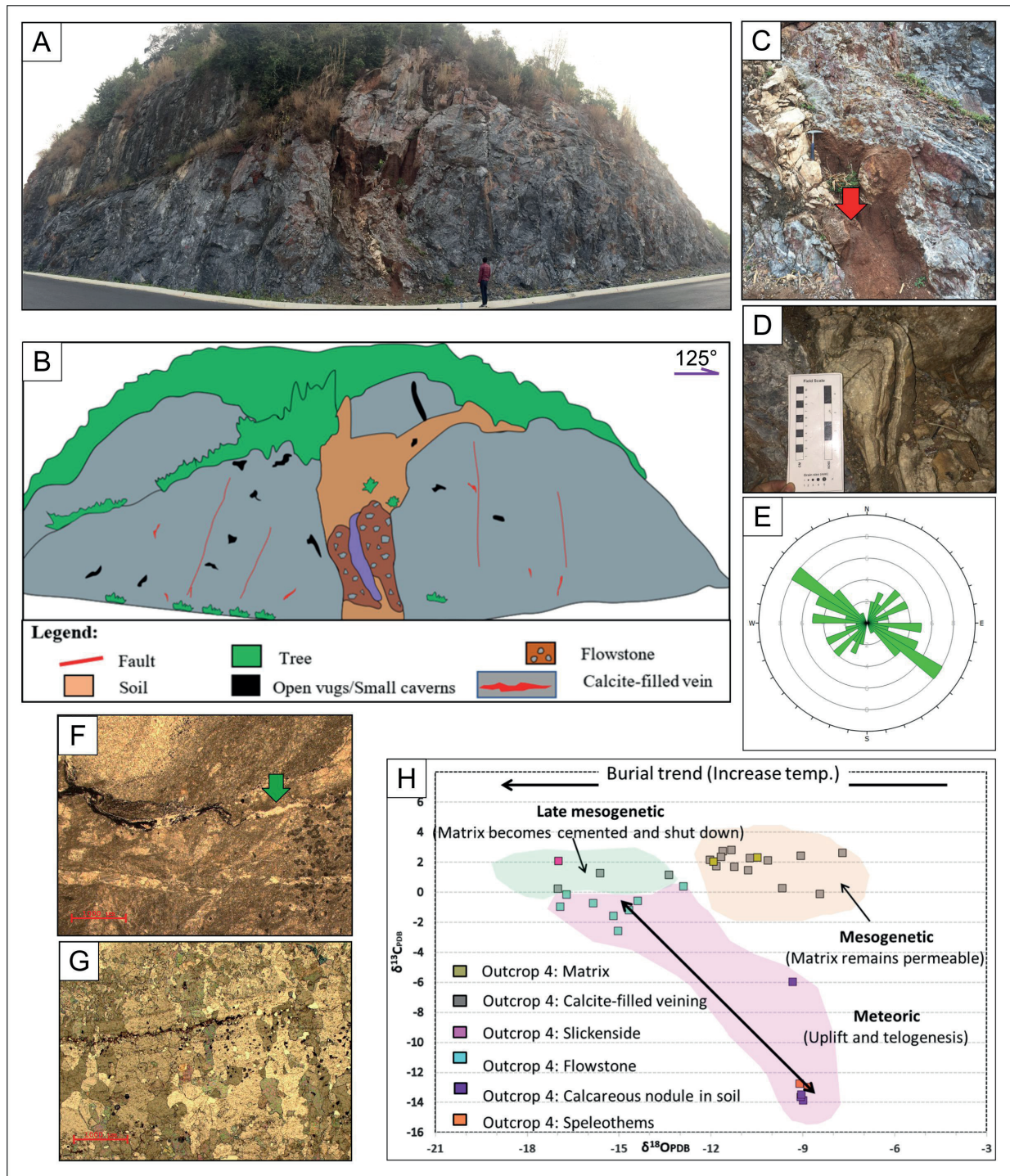


Figure 5. A) & B) Outcrop 4 and its sketch with observed cave, speleothems, and slickenside. **C)** Cavern filled by soil, flowstone with speleothem are observed (red arrow). **D)** Speleothem. **E)** Stereonet shows calcite veins and fractures in studied outcrop trend NW-SE with a minor NE-SW direction. **F)** Fractures filled by sparry calcite (green arrow) with vugs. **G)** Speleothem under microscope. **H)** C-O isotope plot.

On the other hand, the karst overprinted textures show a covariant trend that is typical of a meteoric mixing trend (shaded pink) (Fig. 5H). Speleothems that are precipitated from meteoric water (calcareous nodules and speleothems) show the more negative carbon values and covariant oxygen value that less than $-8\text{\textperthousand}$ to $-9\text{\textperthousand}$. This indicates a fluid-dominated precipitational environment, dominated by rainwater/soil gas derived bicarbonate. Then, there is a group of flowstone values (cyan squares) located on the mixing trend but much closer to the burial spread trend (shaded green) (Fig. 5H). This clustering indicates precipitation from waters supplied with much more bicarbonate coming from dissolved limestone and may be related to a deeper setting than the fluid dominant soils (violet square) with a higher contribution of rock derived fluid. Both clusters on the meteoric mixing trend illustrate the influence of infiltrating groundwater supplying bicarbonate ions flow to precipitation area (Moore, 2001).

5. Discussion

5.1 Fracture systems and calcite cementation and their relationship to regional structure

There are 3 dominant trends of fractures and calcite veins, NE-SW, NW-SE and NNE-SSW, measured in studied areas on Cat Ba island, Northeast Vietnam. The NW-SE and NNE-SSW trends (outcrop 1, 2 and 3), are related to the strike-slip displacements of the Red River fault system (Nguyen et al, 2008).

The NE-SW strike direction are present in outcrops 1 and 4. The density of fractures and calcite veins is high in outcrop 1 and lower in outcrop 4. From thin section analysis, the fractures are identified to be filled by both ferroan and non-ferroan calcite. These NE-SW fractures is considered as being associated with the Yanshanian orogeny, which started some 90Ma ago.

5.2 Diagenetic evolution and its links to poroperm

Two distinct trends are recognized on the $\delta^{13}\text{C}_{\text{PDB}}$ - $\delta^{18}\text{O}_{\text{PDB}}$ crossplot, which can be most clearly seen in outcrop 4 (Fig. 5H): 1) burial trend;

and 2) meteoric mixing trend. The burial trend can be sub-divided into three stages of burial: early, moderate and late stage. The burial stages are indicators of evolving diagenetic processes, from eogenetic to mesogenetic cements in the burial trend (Moore, 2001) while the meteoric mixing trend is an indicator of uplift and exposure (telogenesis).

Earlier burial (eogenetic to early mesogenetic):

In the early to moderate stage of burial, matrix can retain permeability and it has not yet been completely lost by chemical compaction. Both matrix and calcite-filled veins continue to re-equilibrate, bathed by increasingly warmer fluid flows. This is seen in both field observations and isotope covariant plots from the Southeast of the Cat Ba island. It is characterized by sparry calcites and precipitation of siliceous chert nodules; the calcite shows positive $\delta^{13}\text{C}_{\text{PDB}}$ values ($+2\text{\textperthousand}$ to $+3\text{\textperthousand}$) and a gradual increase of $\delta^{18}\text{O}_{\text{PDB}}$ (0\textperthousand to $-8\text{\textperthousand}$) (Fig. 6A).

Mesogenetic signature dominant:

Increasingly negative oxygen illustrates increasing burial depth and temperature. However, in a setting with elevated burial pressure with higher temperatures, if the matrix remains open, fractionation and rock-fluid interaction continue to evolve. This is illustrated by the $\delta^{18}\text{O}_{\text{PDB}}$ value of $-8\text{\textperthousand}$ to $-12\text{\textperthousand}$, which can be observed in all four studied outcrops (Fig. 2H, 3H, 4H, 5H) and is thought to define the time when matrix permeability is ultimately lost. Once matrix permeability is lost isotopic fractionation cannot continue as fluids no longer flow (Warren et al., 2014).

Late mesogenetic signature dominant:

With increasing stress due to deep burial rocks can fracture allowing fluid to flow through, leading to precipitation of calcite with more evolved isotopic signatures. Such fractures can be quickly filled by warmer fluid flows perhaps leading to catagenic dissolution or precipitation of calcite cements. These later cements are indicated by $\delta^{18}\text{O}_{\text{PDB}}$ values greater than $-8\text{\textperthousand}$ to $-12\text{\textperthousand}$

Diagenetic process	Eogenetic	Mesogenetic	Late Mesogenetic	Telogenetic
	Early burial		Late burial	Meteoric mixing
Calcite cementn				
Open fractures				
Dolomitization				
Stylolitization				
Vuggy, solution enhance				
Breccia zone, flowstone				
Speleothem				

Table 2. The relationships between diagenetic processes. The green bars represent reservoir quality enhancement while the black bars represent reservoir quality degradation.

(Fig. 3H, 4H, 5H and Warren et al., 2014). Within this part of the isotope-defined burial trend the values from all four sampled areas overlap (Fig. 6A).

Teleogenetic overprint is defined in the study area by the appearance of caverns, created by regional uplift and created by flows of meteoric waters. In outcrop 4, the sampled cavern is filled by flowstones with rock-dominant meteoric signatures. The uplift is also defined in the C-O isotope crossplot trend (Fig. 5H) from other calcite speleothems with a bicarbonate source more tied to soil gas bicarbonate (more negative carbon values).

In general, all the calcite sampled in the study area indicate a highly complex diagenetic evolution and all current porosity and permeability can be related to diagenetic, not depositional, processes.

5.3 Comparing isotope signatures across studied outcrops and also to carbonate signature in nearby area.

Compared with the rest of the outcrops, outcrop 1 shows a mostly shallower and cooler grouping in the burial trend which is indicated by $\delta^{18}\text{O}_{\text{PDB}}$ values around $-4\text{\textperthousand}$, and $\delta^{13}\text{C}_{\text{PDB}}$ around $+2\text{\textperthousand}$ (blue shaded region) (Fig. 6A). This indicates regional pre-deformation rock fluid burial. It should be noted that only three values for isotope determination are taken from outcrop

1, and broader sampling may widen the crossplot field.

The carbon values of outcrop 2, 3 and 4 (Fig. 6A) show a consistent divergence along burial trend line. The divergence starts when oxygen values are around $-12\text{\textperthousand}$, which is the burial related value, according to Warren et al. (2014), when matrix permeability is lost. Interestingly, in the stage of NW-SE faulting, C-O trends in the outcrop 3 show less negative carbon values than in outcrop 2 (green shaded region) (Fig. 6A). The presence of organic matter residues seen in outcrop 2 suggests a possible catagenic stage (CO_2 evolution), which created more negative carbon values in bicarbonate the fault fluids moving through fractures and veins.

The meteoric mixing trend is well recorded in outcrop 4 (pink shaded region) (Fig. 6A) and it relates with the various karst systems that cut through that outcrop. Meteoric water is considered as a fundamental factor in creating speleothems by precipitation of rainwater/soil gas bicarbonate. In the studied outcrop, the fluid dominant meteoric carbon values are less than 0\textperthousand , with covariant oxygen values that less than $-8\text{\textperthousand}$ to $-9\text{\textperthousand}$. In outcrop 4, uplift that drove the karstification is tied to the Red River fault system. Strike slip movement started in Oligocene-Early Miocene (32-16Ma) and continues until now, and drives some of the tectonic events present in the study area.

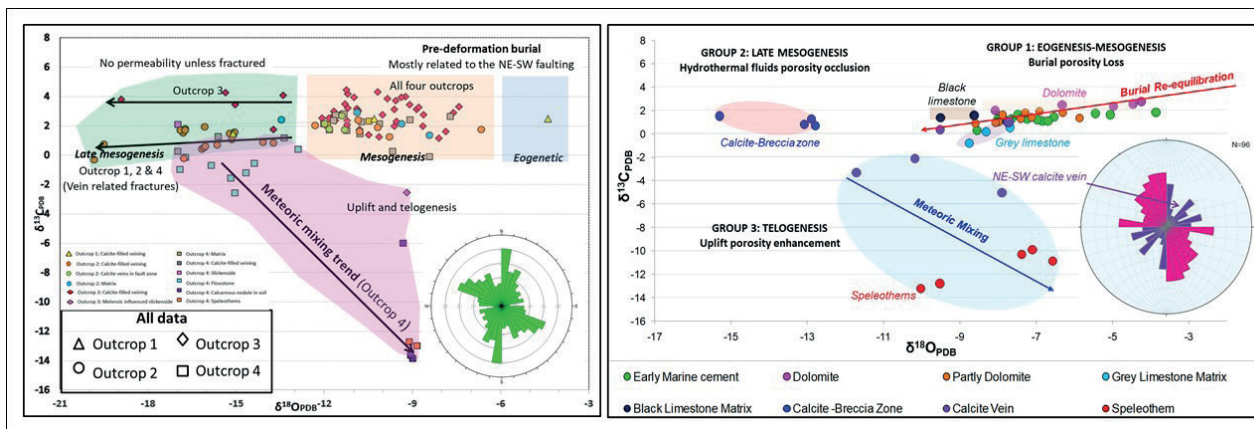


Figure 6. C-O isotope plot illustrating sample values. A) Isotope value in outcrop 1, 2, 3, 4 in the Cat Ba island, Northeast Vietnam. B) Isotope value from previous study in the Northern Vietnam (Nguyen, H. A., 2016).

There are two isotope samples which are taken from slickensides in outcrop 3 and outcrop 4 (Fig. 6A). The isotope value of slickensides from outcrop 3 (pink with diamond shape) is more influenced by meteoric water access, facilitated by recent tectonic activity, probably Red River strike-slip displacement. The isotope value of slickenside in outcrop 4 (pink square) is plotted within the late mesogenetic, which is considered to be related to hotter fluid crossflows, likely in the deeper part of burial trend.

Figure 6B illustrates the isotope-related fracture trends documented in a nearby fractured Devonian carbonate outcrop in the Thuy Nguyen District of Northern Vietnam as published by Nguyen, 2016. The outcrop is located some 80 km from the current study. As on the Cat Ba island, these results show the same burial trend and meteoric mixing trend with similar division of different diagenesis stages. This means that the isotope and fracture results have regional application and so are likely applicable to future exploration wells in the offshore of Northern Vietnam.

6. Conclusion

The main lithology in studied area is a bioclastic muddy limestone with some minor dolomite. Paleozoic carbonates on Cat Ba island are deposited in depositional settings ranging from shallow ramp to marginal basin plain. All these sediments have undergone a complex diagenetic evolution. There are two distinct trends

that can be seen from C-O isotope crossplot, they are 1) the burial trend and 2) the meteoric mixing trend. From very early stages of burial, all of the rocks experienced a consistent set of burial re-equilibration processes, until the oxygen isotope values of the precipitated calcites reached around -12‰. At this point in the burial evolution, matrix permeability is lost (Warren et al., 2014). From then, only tectonically-induced fractures focused the calcite vein precipitates showing even more negative (higher temperature) oxygen values.

There are three main fracture orientations that can be measured in studied outcrop, namely: NE-SW, NW-SE and NNE-SSW. The fracture systems created pathways for fluids to move, which is demonstrated by the calcite filled fractures or calcite filled vugs, followed by uplift and exposure. When the uplift starts, caves and fissures are created with fluid flows focused along pre-existing fractures. This period of calcite precipitation is driven by meteoric mixing, in which speleothems are formed by precipitation of bicarbonate from fluids with high or low rock-fluid levels of interaction. Some flowstone is precipitated from meteoric waters, where more of the bicarbonate come from the dissolution of the rock (less negative carbon values) and not from waters with carbonate coming from the CO₂ in soil gas (more negative carbon values).

Similarly, some slickensides with less negative carbon isotope value either formed in deep burial, contemporaneous with other deep burial

vein calcites, or from fluids related to the dissolution of buried carbonate during early uplift, but with little input from soil gas. If so, the later mechanism indicates the early stages of uplift, as the strata are first fractured by Tertiary age strike-slip faulting. In the most likely scenario, the various meteoric-influenced slickenside calcites relate to Red River strike-slip displacement.

A comparison with results from the nearby outcrops in the Thuy Nguyen district shows that isotope-quantified studies of structure and diagenetic evolution have regional application. As such, future exploration for offshore fractured carbonates in Northern Vietnam should be planned to include a combination of image logs run in the zone of interest tied to isotope analyses of cuttings. Such a combination of techniques would provide an improved understanding of the timing of fractures and the types of fluid present in the subsurface.

7. Acknowledgment

I would like to express my deepest appreciation to my supervisors, Professor John Keith Warren and professor Thasinee Charoentitirat for their guidance and persistent help. Thanks to my family who gave me their love, encouragement and support during my Master's course in Thailand.

8. References

Allegre, C. J., 2008. Isotope Geology. Cambridge University Press, p.512.

Choquette, P. W., & Pray, L. C. (1970). Geologic nomenclature and classification of porosity in sedimentary carbonates. AAPG Bulletin, 54(2), 207-250.

GDGMV. (1993). Geological and mineral resources map of Hai Phong area (Scale 1:50,000). General Department of Geology and Minerals of Vietnam.

Hitzman, M. W., (1999). Routine staining of drill core to determine carbonate mineralogy and distinguish carbonate alteration textures.

Mineralium Deposita, v. 34, 794-798.

Mirzaloo, M., 2013. Depositional and Diagenetic Contrasts between Deep and Shallow Water Successions in the Permian Carbonate of Pak Chong Region, Central Thailand, Chulalongkorn University, (MSc thesis).

Nguyen, H. A., (2016). Characterization of Poroperm Development in a Paleozoic Carbonate Reservoir analog, Northern Vietnam. Bulletin of Earth Sciences, 9, no.2, pp.

Nguyen, N. D., Truong, P. M., & Hiep, H. H. (2008). Structural features and models of water-bearing structure in Cat Ba island. Journal of Geology, 308(2008), A, 49-58.

Tri, T. V., Thanh, T. D., Waltham, T., An, L. D., & Anh, L. H. (2003). The Ha Long Bay World Heritage: Outstanding geological values. Journal of Geology, 22, B, 1-18.

Warren, J. K., Christopher, K. Morley, Charoentitirat, T., Cartwright, I., Ampaiwan, P., Khositchaisri, P., Yingyuen, J. (2014.). Structural and fluid evolution of Saraburi Group sedimentary carbonates, central Thailand: A tectonically driven fluid system. Marine and Petroleum Geology, 55, 100-121. Retrieved December 24, 2014, from www.elsevier.com/locate/marpetgeo.